

Article

Evaluation of Facial Skin Condition Based on RBX Image Technology

Patrick Po-Han Huang¹, Shu-Chen Chang² and Chih-Yu Wang^{3,*}

¹ Huang PH Dermatology and Aesthetics, Kaohsiung, Taiwan; skindr.huangph@gmail.com

² Department of Hospitality Management, Tajen University, Pingtung, Taiwan; doris@tajen.edu.tw

³ Department of Biomedical Engineering, I-Shou University, Taiwan;

* Correspondence: crab@isu.edu.tw

Received: May 9, 2022; Accepted: Jun 9, 2022; Published: Jun 30, 2022

Abstract: The skin color of the human face is mainly determined by the content of hemoglobin (in red) and melanin (in brown). RBX image technology transforms full-color images into RBX color space, in which the "Red" component is associated with hemoglobin, and the "Brown" component is associated with melanin. This article presents a skin condition evaluation system based on RBX image technology, which is practically applied to the identification of the severity of rosacea patients, as well as the whiteness of the skin of the patient receiving pulse laser toning. In the research of rosacea grading, we analyze the "Red" component image and establish the R-G index to grade the severity of rosacea. It was found that the value of the R-G index increased with the severity of rosacea. ANOVA test results show significant differences among the four severity groups. In the research on the effect of facial skin toning by pulsed laser, we analyzed the "Brown" component image and established five brightness levels as indicators to evaluate the skin whitening effect. The result shows that the ups and downs of these brightness levels reflect changes in skin tone. These indicators provide a new way for quantification of skin conditions.

Keywords: RBX image technology, Rosacea severity, Picosecond laser toning, R-G index, Brightness level

1. Introduction

To evaluate the facial skin condition for medical purposes, digital images are taken to quantify the skin tone for computer analysis. In general, images are decomposed into three primary color palettes of red (R), green (G), and blue (B) for computer analysis. However, skin tone is mainly determined by two substances: hemoglobin and melanin [1,2]. Therefore, decomposing images into RGB patterns is not able to effectively correspond to the main factors: hemoglobin and melanin. Demirli et al. proposed an RBX color space to represent the color produced by the two substances on the skin for obtaining accurate skin tone information.

The RBX image technology was proposed by Canfield Imaging Systems, United States. The principle is to decompose the original full-color image into RBX color space, including the red component image (representing the scattering spectrum of hemoglobin), the brown component image (representing the scattering spectrum of melanin), and the X component (undefined and not being used) [3]. **Fig. 1** shows a schematic diagram of the transformation of the RGB color space to RBX. A full-color cross-polarized image was decomposed into Red and Brown components. The Red component indicates the distribution of hemoglobin in the skin, while the Brown component indicates the distribution of melanin in the skin. Since hemoglobin and melanin are distributed on the surface and deep of the skin, a polarized light source must be used when taking pictures to obtain the scattered light of hemoglobin and melanin at different depths and avoid the interference of specular reflection (**Fig. 2**).

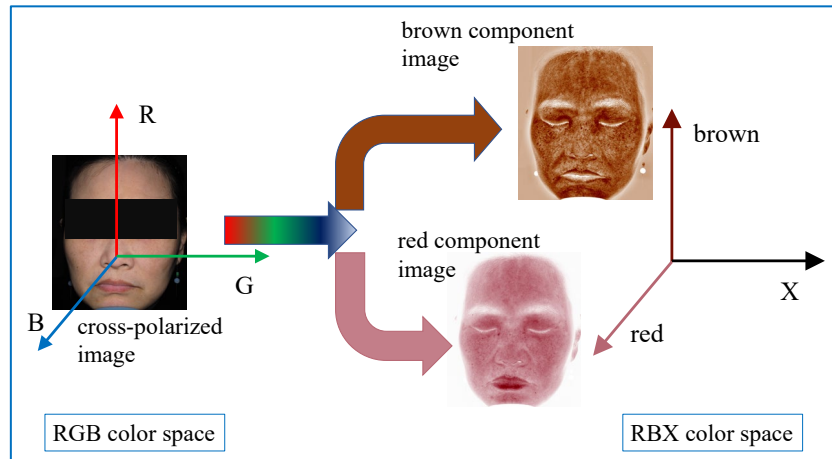


Fig. 1. Schematic diagram of transformation between RGB color space and RBX color space.

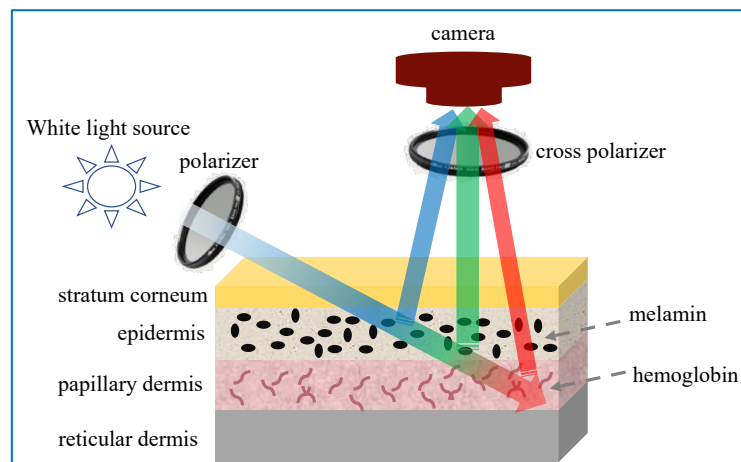


Fig. 2. Using a pair of cross polarizer to obtain scattered light of melanin and hemoglobin in deeper skin1.

Rosacea is a common chronic skin disease that usually occurs on the face, especially the forehead, cheeks, chin, and lower part of the nose. It is characterized by persistent or repeated erythema on the skin, accompanied by dilation of microvessels, and even papules or pustules. In severe cases, it not only affects the appearance but also causes discomfort or pain to the patient. The severity of rosacea often affects the treatment strategies adopted by physicians, so how to correctly grade it is an important issue for treatment of rosacea. At present, the most widely used grading system for rosacea was proposed by Plewig et al. [4], in which the severity of rosacea was divided into three grades based on clinical symptoms.

The grading system qualitatively describes the symptoms of rosacea. However, based on the clinic experience and the research of Gessert et al. [3], it is not easy to apply the system into practice due to the difficulties to quantify for assessing the severity of rosacea and for tracking the progress of treatment. In order to establish a grading rule for rosacea, Bamford et al. conducted a study to analyze the correlation between the severity grading of 82 patients with rosacea by four dermatologists, and the various symptoms of rosacea (including erythema color, papules/pustules, and hyperplasia of skin tissue). It was found that changes in erythema color had the highest correlation with severity classification, whether on the whole face, forehead, cheeks, nose, or chin[5]. Tan et al. studied the internal (intra-raters) and external (inter-raters) reliability of the Clinician Erythema Assessment grading scale (CEA) for rosacea (Table 1). The five-point method was found to be reliable for the classification of rosacea [6]. The above studies show that it is feasible to judge the severity of rosacea by the color of the erythema.

Table 1. Clinician Erythema Assessment (CEA) scale[6]

	CEA
0 = Clear	Clear skin with no signs of erythema
1 = Almost clear	Almost clear; slight redness
2 = Mild	Mild erythema, definite redness
3 = Moderate	Moderate erythema; marked redness
4 = Severe	Severe erythema; fiery redness

Experienced physicians can evaluate the severity of rosacea by visually inspecting the color of erythema. However, individual differences are inevitable for each physician. Furthermore, there is still no standard training model for junior physicians. Therefore, developing standardized measurement and analysis tools for grading the severity of rosacea is necessary for physicians and researchers [5]. Several quantitative techniques have also been developed for the identification of rosacea severity, such as reflection confocal microscopy (RCM), dermoscopy, capillary microscopy, optical coherence tomography (OCT), ultrasonography, and thermal imaging [7]. Since a large amount of Demodex may cause rosacea, RCM and OCT are used to monitor Demodex in the skin of rosacea patients [8]. Rosacea is an inflammatory phenomenon that causes telangiectasia. Therefore, monitoring the telangiectasia of rosacea lesions with dermoscopy and capillary endoscopy can be used as a quantitative indicator of the severity of rosacea [9]. In addition, photoacoustic imaging as a high-resolution hemodynamic measurement tool has been applied as a new tool to measure microvascular changes and has good potential in monitoring skin inflammation and cancer [10]. From the above description, it is found that a rosacea severity assessment tool using a non-invasive method is worth developing. Being compared with other methods, RBX image technology is the most cost-effective for the development of the grading system.

In recent years, there have been good results in the study of skin conditions using digital image analysis methods [11,12]. Binol et al. used Ros-NET to develop a deep learning model for rosacea classification to automatically detect the location of rosacea [13]. Pan et al. used the VISIA system (Canfield Scientific, Parsippany, NJ, USA) for image acquisition and analysis. It was found that the Red component image obtained by RBX conversion had the best correlation with the rosacea grade obtained by the CEA system [14]. The research results verify that the color change of rosacea is the best grading index of rosacea.

Asians have brown skin so the color of facial erythema is apt to be concealed, which affects the classification and diagnosis of rosacea. In this study, the RBX image technology was used to transform the original image into the Red component to reduce the effects of brown skin. Then, we established a mathematical model as a quantitative indicator of the severity of rosacea. In addition, we adopted the Brown component (also transformed RBX image technology) to establish a mathematical model to quantify the skin tone after 755 nm picosecond laser toning treatment. A mathematical model was then established to evaluate the skin whitening effect.

2. Materials and Methods

The format of the color image is mostly composed of RGB color vector spaces (red, green, and blue). However, the color of main chromophores in the skin such as hemoglobin and melanin cannot be precisely represented by RGB color space. On the other hand, the RBX image technology decomposes the full-color image into the Red component image (representing Hemoglobin) and the Brown component image (representing melanin). This allows researchers to select images of the Red or the Brown components for analysis.

Photographs were taken with a skin imaging camera (Reveal Imager, Canfield Scientific, Inc., Fairfield, NJ, USA) (**Fig. 3**) under non-polarized light and polarized light. The former presents the skin condition when viewed visually, while the latter eliminates the effects of reflections and capture deeper skin images [15].



Fig. 3. Reveal Imager (Canfield Scientific, Inc., Fairfield, NJ, USA) [16].

3. Results

3.1. Rosacea severity identification based on RBX image technology

89 polarized images of patients (including 8 normal, 16 mild, 37 moderate, and 28 severe rosacea) were collected for analysis. The severity of rosacea was graded by two dermatologists. Photographs of patients were transformed into the "Red" component images and the "Brown" component images by using RBX image technology. Since the color of the rosacea tended to be red, we used the "Red" component image for analysis. Fig. 4 shows the original cross-polarized images, and "Red" component images (transformed by RBX image technology) and the RGB histogram of the "Red" component images. Fig. 4(a)-(d) represent normal, mild, moderate, and severe rosacea, respectively.

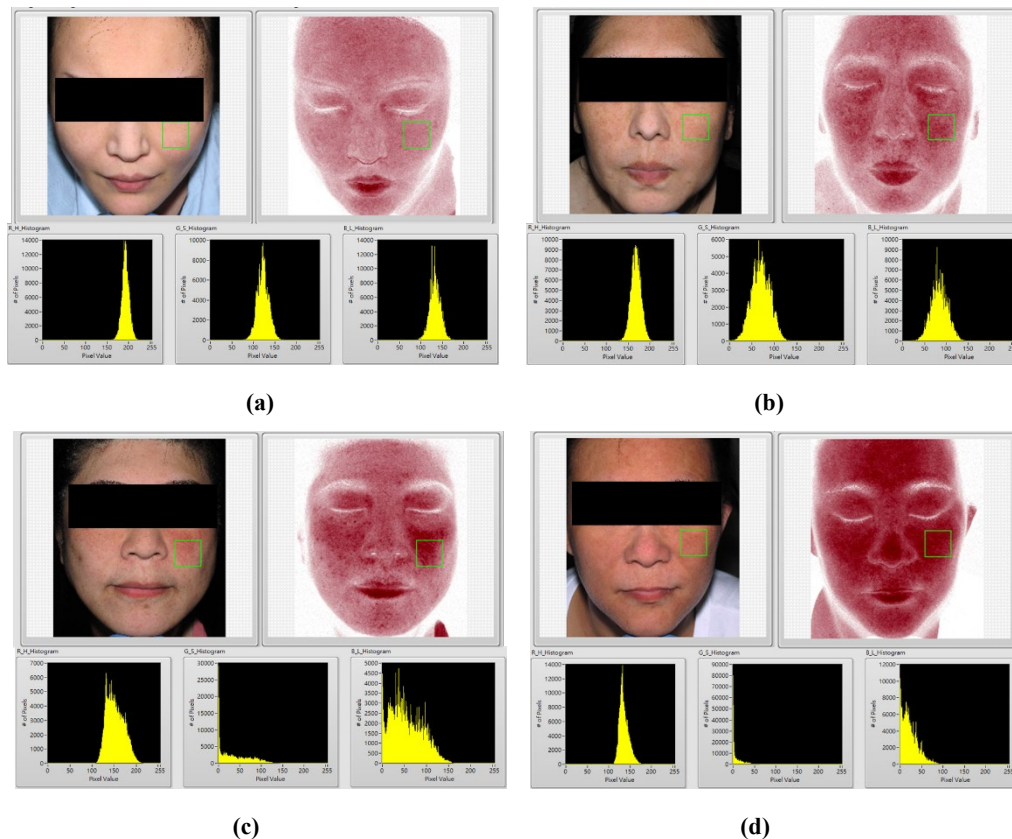


Fig. 4. Full-color polarized images, "Red" component image transformed by RBX image technology, and RGB histogram of "Red" component images. (a) normal; (b) mild rosacea; (c) moderate rosacea; (d) severe rosacea.

As shown in Fig. 4, the normal facial skin image appears lighter red. The more severe the rosacea, the darker the red is. The analysis process is described as follows: First, a dermatologist selected a square "region of interest (ROI)" on each polarized image. The ROI at the same position was selected on the "Red" component image transformed by the RBX image technology. The selected ROI was decomposed into an RGB palette, and the individual histograms (brightness in the horizontal axis and the number of pixels

in the vertical axis) were calculated. The result showed that the intensity distribution of the “red” histogram was the highest with normal skin color (a mean value of about 200), and decreased with the severity of the rosacea (a mean value of about 150). The “green” histogram showed similar results but more obvious trend. Based on the above observations, we adopted the (R-G) index to identify the severity of rosacea with the following equation.

$$(R - G)_{index} = \frac{\sum_{i=0}^{255} i \cdot n_{ri}}{\sum_{i=0}^{255} n_{ri}} - \frac{\sum_{i=0}^{255} i \cdot n_{gi}}{\sum_{i=0}^{255} n_{gi}} \quad (1)$$

where n_{ri} is the number of pixels of the brightness value i in the red histogram, and n_{gi} is the number of pixels of the brightness value i in the green histogram.

89 patients were divided into 4 groups (8 normal, 16 mild, 37 moderate, and 28 severe rosacea) according to the identification of the physician, and their (R-G) indexes were calculated and averaged. Fig. 5 shows the mean values of the (R-G) index in 4 groups. Normal patients had the lowest (R-G) index value. The value of the (R-G) index increases with the degree of rosacea severity. An ANOVA test result showed that there were significant differences among the (R-G) index of the four groups ($p < 0.05$). Thus, it is feasible to classify the severity of rosacea with RBX image technology.

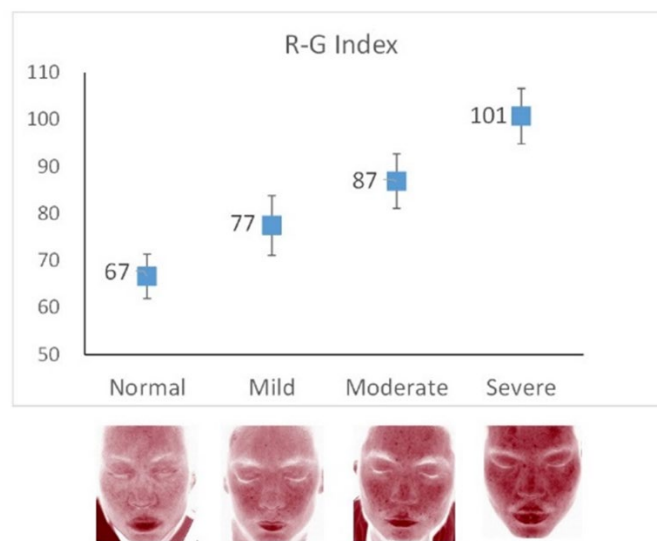


Fig. 5. Average R-G index of patients with four groups (normal, mild, moderate, and severe rosacea).

3.2. RBX image technology to evaluate the effect of picosecond laser toning

The degree of facial whitening is determined by the melanin content in the skin. A laser with appropriate wavelength and energy destroys the melanin in the skin and achieves the effect of skin cleansing. Here, the RBX image technology is used to transform the polarized image into the "Brown" component images and quantify the degree of skin whitening. In this study, the facial skin of the patient who underwent 755 nm picosecond laser toning on the cheek was evaluated for the whitening effect after treatment. First, the polarized image of the patient was transformed into the "Red" and "Brown" component images by using RBX image technology. Then, the “Brown” component image was used for analysis to evaluate the effect of facial whitening.

Fig. 6 shows the “Brown” component image, the grayscale image of the “Brown” component image, and the histogram of the grayscale image. we grouped the histogram into five levels, namely Level 0 (with the brightness of 5–54), Level 1 (with the brightness of 55–104), Level 2 (with the brightness of 105–154), Level 3 (with the brightness of 155–204), Level 4 (with the brightness of 205–254). The proportion of the pixel number in each level was calculated with Eq. (2).

$$Level\ i = \frac{\sum_{k=5}^{54} n_{k+i:50}}{\sum_{l=5}^{254} n_l} \quad (2)$$

where n_m represents the number of pixels with brightness m in the histogram. Here we named it "brightness level".

Fig. 6(a) shows the results before laser treatment. From the normalized histogram, we found that the proportion of Level 2 was the highest, followed by Level 3. This indicated that the skin tone tended to be dark before laser treatment. Fig. 6(b) shows the

results of the 7th day after the second laser toning. The proportion of Level 3 increased to slightly higher than that of Level 2. The skin tone became whiter than that before laser treatment. **Fig. 6(c)** shows the 21st day after the second laser toning. The proportion of Level 3 was much higher, surpassing that of Level 2. This suggests that the face tone was more whitened before laser treatment.

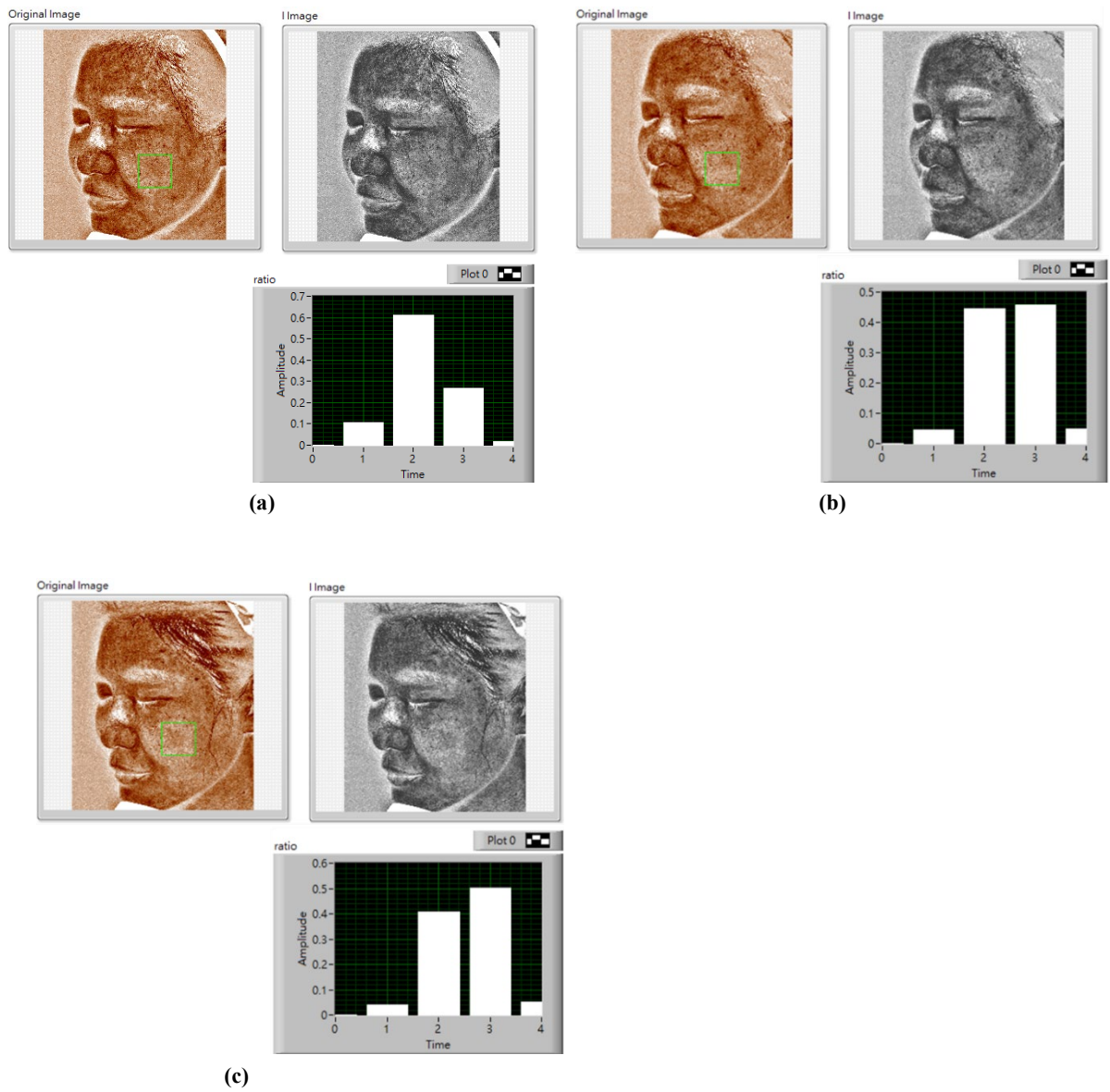
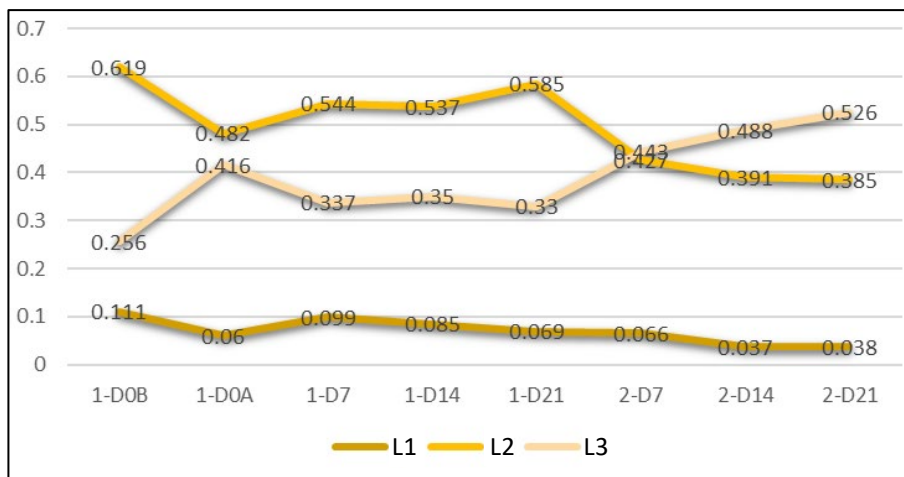


Fig. 6. Whitening effect after 755 nm picosecond laser toning. (a) Result before picosecond laser toning; (b) Result of the 7th day after 2nd picosecond laser toning; (c) Result of the 21th day after 2nd picosecond laser toning.

Fig. 7 shows the changes from Level 1 to Level 3 with time after 755 nm picosecond laser toning. At 1-D0B (before the first laser treatment), the patient showed original skin tone. The value of L1 (0.619) was about 2.4 times higher than that of L2 (0.256), indicating a darker skin tone. After laser treatment (1-D0A), L2 decreased (0.482), while L3 increased (0.416), indicating a whiter skin tone. However, for 1-D7, 1-D14, and 1-D21, the skin tone slowly returned to darker over time. At 1-D21 (the 21st day after the 1st laser treatment), the L2 reached a high point (0.585), while the L3 reached a low point (0.33). The patient, therefore, received the 2nd laser toning at 1-D21. At 2-D7 (7th day after 2nd laser treatment), the value of L2 decreased significantly (0.443), and the value of L3 increased (0.427), showing a cross of the value. After that, L2 kept decreasing while L3 kept increasing. At 2-D21 (the 21th day after 2nd laser treatment), the L2 reached a low point (0.385), while the L3 reached a high point (0.526). The above results showed that the skin tone could not be quantified using the normalized histogram technology.

Fig. 7 The changes of Level 1 to Level 3 with time after 755 nm picosecond laser toning



4. Conclusions

In this research, the RBX image technology was used to transform cross-polarized images into the "Red" component images and the "Brown" component images, which were then adopted to develop skin condition identification systems for patients with rosacea or receiving laser whitening treatment. The results showed that the system was effective for skin condition identification. In the future, we will collect more subjects for analysis to improve the effectiveness of this system.

Author Contributions: Dr. Huang provided equipment and filmed images. Prof. Wang and Prof. Chang performed data analysis. Prof. Wang wrote the original draft of this article. Dr. Hhang, Prof. Wang, and Prof. Chang reviewed and edited it.

Funding: This research did not receive external funding.

Conflicts of Interest: The authors declare no conflict of interest.

References

- Liu, Z.; Zerubia, J., Melanin and hemoglobin identification for skin disease analysis, 2013 2nd IAPR Asian Conference on Pattern Recognition, IEEE, **2013**, 145–149.
- Zonios, G.; Bykowski, J.; Kollias, N., Skin melanin, hemoglobin, and light scattering properties can be quantitatively assessed in vivo using diffuse reflectance spectroscopy, *Journal of Investigative Dermatology*, **2001**, 117(6), 1452–1457.
- Demirli, R.; Otto, P.; Viswanathan, R.; Patwardhan, S.; Larkey, J., RBX® technology overview, Canfield Systems White Paper (2007).
- Plewig, G.; Kligman, A.M., Acne and rosacea, Springer Science & Business Media 2012.
- Bamford, J.T.; Gessert, C.E.; Renier, C.M., Measurement of the severity of rosacea, *Journal of the American Academy of Dermatology*, **2004**, 51(5), 697–703.
- Tan, J.; Liu, H.; Leyden, J.J.; Leoni, M.J., Reliability of clinician erythema assessment grading scale, *Journal of the American Academy of Dermatology*, **2004**, 71(4), 760–763.
- Logger, J.; de Vries, F.; van Erp, P.J.; de Jong, E.; Peppelman, M.; Driessen, R.; Noninvasive objective skin measurement methods for rosacea assessment: a systematic review, *British Journal of Dermatology*, **2020**, 182(1), 55–66.
- Liang, H.; Randon, M.; Michee, S.; Tahiri, R.; Labbe, A.; Baudouin, C., In vivo confocal microscopy evaluation of ocular and cutaneous

- alterations in patients with rosacea, *British Journal of Ophthalmology*, **2017**, *101*(3), 268–274.
9. Sgouros, D.; Apalla, Z.; Ioannides, D.; Katoulis, A.; Rigopoulos, D.; Sotiriou, E.; Stratigos, A.; Vakirlis, E.; Lallas, A., Dermoscopy of common inflammatory disorders, *Dermatologic Clinics*, **2018**, *36*(4), 359–368.
 10. Attia, A.B.E.; Moothanchery, M.; Li, X.; Yew, Y.W.; Thng, S.T.G.; Dinish, U.; Olivo, M., Microvascular imaging and monitoring of hemodynamic changes in the skin during arterial-venous occlusion using multispectral raster-scanning optoacoustic mesoscopy, *Photoacoustics*, **2021**, *22*, 100268.
 11. di Ruffano, L.F.; Takwoingi, Y.; Dinnes, J.; Chuchu, N.; Bayliss, S.E.; Davenport, C.; Matin, R.N.; Godfrey, K.; O'Sullivan, C.; Gulati, A., Computer-assisted diagnosis techniques (dermoscopy and spectroscopy-based) for diagnosing skin cancer in adults, *Cochrane Database of Systematic Reviews*, **2018**, *12*.
 12. Tan, J., Evaluating rosacea noninvasively and objectively, *British Journal of Dermatology*, **2020**, *182*(1), 10–11.
 13. Binol, H.; Plotner, A.; Sopkovich, J.; Kaffenberger, B.; Niazi, M.K.K.; Gurcan, M.N., Ros-NET: A deep convolutional neural network for automatic identification of rosacea lesions, *Skin Research and Technology*, **2020**, *26*(3), 413–421.
 14. Pan, Y.; Jia, K.; Yan, S.; Jiang, X., Effectiveness of VISIA system in evaluating the severity of rosacea, *Skin Research and Technology*, 2022.
 15. Matsubara, A., Differences in the surface and subsurface reflection characteristics of facial skin by age group, *Skin Research and Technology*, **2012**, *18*(1), 29–35.
 16. Yeomans, M., Canfield designs 'Reveal imager' to generate more business for skin care specialists, 2012. <https://www.cosmeticsdesign.com/article/2012/04/30/canfield-designs-reveal-imager-to-generate-more-business-for-skin-care-specialists>. (2022).

Publisher's Note: IJKII stays neutral with regard to jurisdictional claims in published maps and institutional affiliations.

Copyright: © 2022 The Author(s). Published with license by IJKII, Singapore. This is an Open Access article distributed under the terms of the [Creative Commons Attribution License](https://creativecommons.org/licenses/by/4.0/) (CC BY), which permits unrestricted use, distribution, and reproduction in any medium, provided the original author and source are credited.